Journal of the Serbian Chemical Society
JSCS-info@shd.org.rs • www.shd.org.rs/JSCS
J. Serb. Chem. Soc. *88* (3) 267–281 (2023)
JSCS–5625
Original scientific paper
Published 27 January 2023

Formation of intermediate gas–liquid system in aromatics' thin layers

ROSTISLAV V. KAPUSTIN[1], IOSIF I. GRINVALD[1]*, ANDREY V. VOROTYNTSEV[2], ANTON N. PETUKHOV[2,3], VLADIMIR M. VOROTYNTSEV[1], SERGEY S. SUVOROV[2] and ALEXANDRA V. BARYSCHEVA[2]

[1]*Alekseev State Technical University of Nizhny Novgorod, Nizhny Novgorod, Russia,* [2]*Lobachevsky State University of Nizhny Novgorod, Nizhny Novgorod, Russia and* [3]*Dmitry Mendeleev University, Moscow, Russia*

(Received 3 October, revised 25 November, accepted 9 December 2022)

Abstract: The present work discusses IR spectroscopic experiments and quantum-chemical DFT study of structure and intermolecular binding in the intermediate gas–liquid systems of aromatics, namely, benzene, furane, pyridine and thiophene. These systems can be generated in thin layers near a solid surface by two different methods, depending on the physical properties of the sample. The first method includes evaporation with a subsequent compression of a sample in an optical cell of variable thickness, and it is applied to volatile components: benzene, furane, thiophene. For benzene and pyridine the second method is used, which involves a heating-initiated evaporation into a closed inter-window space with an after-cooling of a sample. It was shown that the formed layer is not an adsorbate or a condensate. The IR data obtained by these two methods lead to conclusion that the given systems of the considered aromatics manifest dual gas–liquid spectral properties which can change each into other by varying external conditions. According to the DFT calculation results, the spatial arrangement in the aromatic thin layers can be described as a combination of π- and σ-bonded clusters, which simulate the gas and the liquid phase state properties.

Keywords: fluid-like; intermediate phase; IR spectroscopy; DFT calculations.

INTRODUCTION

The concept of thin layers in the near-surface area was mentioned in the works of Ananikov's group, which deal with the mechanisms of heterogeneous catalysis.[1] This term primarily refers to catalytically active metal particles, and it can mean both a nanoscale layer and molecular clusters. However, later it was shown that the very concept of the thin layer has a much wider application. The

* Corresponding author. E-mail: grinwald@mts-nn.ru
https://doi.org/10.2298/JSC211003087K

thin-layer effect was observed in different phase states of organic liquids: in a solid-film-encapsulated form, in a thin-layer liquid on a solid surface, in dense vapours near a solid surface, and also in a low-temperature matrix.[2]

Various theoretical and experimental methods for studying transient thin-layer systems have been suggested, including *ab initio* DFT calculations in the Gaussian software package (B3LYP 6–311++G [2d, 2p] basis set), which make it possible not only to optimize the geometry of molecular clusters, but also to compare theoretical IR vibrational spectra with experimental ones directly.[3] However, the available computing schemes does not allow to calculate the entire supramolecular system in all its complexity and heterogeneity, being limited only to isolated clusters. Therefore, only the experimental *in situ* IR spectral methods for studying organic-compound thin layers make it possible to reveal their unique phase properties and make assumptions about their spatial structure.[4]

The structure and properties of the thin layers can vary and manifest themselves differently depending on the method of generation, the state of aggregation, and the class of the compound, as well as the types of intermolecular interaction prevailing in it. For example, in liquid chlorocarbons, chlorine acts as the main binding particle for gaseous clusters' and condensed supramolecular structures. Accordingly, tetrachloromethane forms the most stable thin-layer gas-phase system among them. The unusual intermolecular properties of tetrachloromethane were predicted in the spectral study.[5] There was shown that gas-phase tetrachloromethane exists not only in the single molecular shape that has T_d symmetry, but also in the transformed shape having C_{3V} symmetry. This speculation was confirmed by the spectra of gaseous tetrachloromethane at various temperatures. It was resumed that the pyramidal structure relates to the cluster shape, where the chlorine atom provides the binding between molecules. The chlorine atom shift in the cluster can occur owing to the association of the molecules. It leads to the transformation of the molecular geometry to the almost planar D_{3h} symmetry, in which A_1 stretching band is forbidden in IR spectra. The above interpretation of the liquid chlorocarbons' IR spectral data based on the symmetry point groups' theory showed the appearance of two structural modifications – the pyramidal C_{3V} and the biplanar D_{2h} or D_{2V} symmetry. The DFT calculations also predicted the transformation of the initial isomer into biplanar and pyramidal ones. Thus, it was concluded that the phase characteristics in chlorocarbons can be combined: in the gas phase, some interactions resembling liquid ones may retain, and *vice versa*.

The most unusual and chemically resistant form of the studied thin layers are solid-phase chlorosilane films with an encapsulated liquid, generated in an argon atmosphere – they are able to selectively protect the internal component, preventing its air hydrolysis (which could be explosive),[6] but allowing slow oxidation

over months, which was repeatedly confirmed by IR spectroscopy and electron microscopy data.[7]

Systems that combine gaseous and liquid physicochemical properties are known as supercritical fluids (SCF).[8] They can dissolve large volumes of gases and mix indefinitely with each other. In addition, a slight adjustment of pressure and temperature within the limits of supercritical values makes it possible to influence the density of the SCF and its other parameters to such an extent that, in the phase diagram, the SCF is even conditionally divided into gas-like and liquid-like states. Although there is actually no clear boundary between these two states, many researchers conditionally draw it along the so-called Widom line, the transition through which is described by the term pseudo-boiling, which once again emphasizes the variability degree of the SCF physicochemical properties under changing external conditions. One of the most reliable methods for tracking such phase transformations is considered to be IR spectroscopy, since it allows one to unambiguously assign some individual characteristic bands to the gas or liquid phase and thus clearly distinguish between the gas and liquid properties of the sample.[9] In the thin layers of chloromethanes and chloroethanes, it was possible to reproduce the main properties of SCF. Specifically, in the IR spectra, two separate phases – gas-like and liquid-like – were distinguished by their manifestation in the characteristic bands that change a shape depending on the phase state of the substance. Similar to the SCF, in the thin layers these states smoothly and continuously change each into other with a slight adjustment of pressure and temperature. Depending on the boiling point of the component, under ambient conditions it may appear in the thin layers more as a gas-like or liquid-like one.[10] It is important to note that the terms “gas-like” and “liquid-like” used in the thin-layer system description are not accidental or intended to emphasize the similarity of a given state with a fluid. The states observed by IR spectroscopy are in fact neither a real gas nor a real liquid, but only exhibit some of their spectral properties, which is easy to prove: it is almost impossible to obtain the IR spectrum of a real gas at an equilibrium vapor pressure in the thin spectral cell (1–6 mm).

As already mentioned, the properties of thin-layer gas–liquid systems are largely determined by the types of intermolecular bonding. For this reason, the compounds with aromatic properties, both proper hydrocarbons and heterocycles, are of particular interest for study since they are distinguished from the other previously studied organic compounds by their intermolecular interactions. Back in the 70s Shakhparonov, who predicted the existence of the specific interactions in the non-polar hydrogen-bonded liquids, suggested the formation of molecular π-complexes (molecular stacks) between aromatic rings.[11] Later, this concept was confirmed and developed by Abramovich’s group.[12–14] The single benzene molecule geometry is usually taken as a planar ring. This geometry corresponds

to D_{6h} symmetry point group; according to the selection rules, only one stretching C–H band (E-specie) should be active in its IR spectra. Nevertheless, in the real liquid benzene spectra there are three bands, and in the solid benzene there are even four bands in C–H stretching region. Three bands that have isotopic H/D shift close to the theoretical prediction also are observed in benzene-d_6 spectrum. This spectral picture is assigned to the existence of two molecular forms in the liquid phase: a planar shape, in which one IR band is active (D_{6h} symmetry), and a shape with two IR bands (A_1- and E-species), corresponding to the C_{3V} symmetry. Assumedly, the benzene molecule exists in the liquid state as a cluster system, where C–H bonds deviate from the ring plane to the neighbouring molecule, which leads to a distortion of the C–H stretching vibrations' symmetry.[15]

In solution of dichlorobenzene, there are strong neighbouring-molecule interactions between chlorine atom and carbon in the aromatic ring and between carbon atoms as well. Since the arrangements of molecules in a crystal always correspond to the potential energy minima of the system, it can be used to verify the results of molecular light scattering experiments combined with modelling procedure and consequently reveal the structure and characteristics of the mutual arrangement in molecules as well as the intermolecular binding types in the liquid phase.[16]

A structural element that determines the molecular arrangement in the benzene liquid phase, was earlier presented as a set of dimers that have several geometry configurations. Later, the trimers were considered as a formed element in the stack model of the benzene liquid phase. The conducted DFT calculations with different transformations of the initial molecular geometry predict that the optimal configuration is the stack with a chair shape of the central and two planar rings; the trimers are bonded in a spatial structure by the hydrogen bridges.[17] This concept explained the IR data outside the scope of traditional assignment. In the trimer spectrum, a C–H stretching band assigning to both planar rings should be observed while the C–H central-ring stretching exhibits two bands: the first one assigns to a pair of equivalent (C_1–H_1) and (C_4–H_4) bonds, and the second one – to a quartet: (C_i–H_i), i = 2.3 or 5.6. The stretching bands of the hydrogen bridges shift in the middle IR region due to the mixing of the C–H and C–C stretching. Consequently, there is a pair of bands that corresponds to two bridging C–H bonds' stretching in the stacks bound in two mutually perpendicular plains, as it was shown earlier.[18]

Based on the data presented above, it can be stated that the formation mechanism of the thin-layer systems with dual gas–liquid phase characteristics is caused and provided by the intermolecular binding. Using the example of chlorocarbons and chlorosilanes, one can see how the properties of the thin layers change depending on the supramolecular geometry. The formation of certain stable structures with unusual phase properties indirectly confirms the presence

of nonstandard intermolecular binding, which is realized through such structures. Thus, the experimental studies of the thin aromatic layers considered in the present work are intended to find a new and more reliable confirmation of the above assumptions about the supramolecular geometry of aromatics. If the intermolecular binding is indeed the thin-layer systems' basis, then the properties of such systems for aromatics should differ from chlorides to the same extent as their supramolecular characteristics do. Pure benzene, a common organic solvent that can be directly compared with liquid chlorocarbons, is studied as a typical representative of aromatics. Moreover, it is very promising to study heterocycles, which are known to have some aromatic properties as well. Below we consider the question of whether there are some heterocyclic intermolecular interactions, and are they the reason the characteristics of their thin-layer systems differ from those of benzene. In order to clearly distinguish between the proper aromatic properties, which manifest themselves to the same extent in various heterocycles, from the intermolecular interactions of the heteroatom itself, which change depending on the compound, we have selected three aromatic heterocycles with different heteroatoms: thiophene, furane and pyridine. The main objective of the work is to study the four selected substances under conditions as close as possible to those in which the chlorides were considered, for the most accurate comparison. As a part of the presented work, we have concluded an extensive quantum-chemical study based on the DFT calculations, which is also expected to complement the earlier theoretical studies of chlorocarbons with the data on intermolecular binding in the aromatics and allow the quantum chemical model of the gas–liquid thin-layer system structure to be evaluated for the varied classes of compounds in terms of DFT study.

EXPERIMENTAL

In the present work, as mentioned above, four components were studied: benzene, thiophene, furane and pyridine. The optimal parameters for thin-layer gas-liquid systems' generation (evaporation time, τ, cell type, heating temperature, T and boiling point, T_B) depend on the individual properties of each component, primarily its boiling point, as shown in the Table I.

TABLE I. The optimal parameters for the selected compounds' transient state formation

Compound	τ / min	Cell type	T / K	T_B / K
Benzene	60	VTOC/MCOH	295/323	353
Thiophene	60	VTOC	295	357
Furane	25	VTOC	295	304
Pyridine	10	MCOH	363	389

For the selected components, whose intense evaporation do not require additional heating, a Perkin–Elmer variable-thickness optical cell was applied (here we use the abbreviation VTOC). This method was described in detail in the earlier paper.[10] The formation of the dual gas-liquid thin-layer system occurred under the compression-extension procedure of the cell

inter-window distance from 6 to 1 mm and in reverse. The optimal evaporation time required for the gas–liquid state formation depends on the boiling point of compound and varies from 25 to 60 min.

The effect of the thin gas-liquid layers generation for benzene and low-volatile pyridine has been achieved by the method of evaporation of liquid sample placed between optical window in following way. The sample drops (Fig. 1, 1) on the edge of a KBr optical window (Fig. 1, 2) so that to prevent its falling into the IR optical beam (Fig. 1, 3) under a Teflon® 1-mm--thickness gasket (Fig. 1, 4), covering them from above with another optical window (Fig. 1, 5). Then both windows with a gasket between them are placing and clamping in a manual collapsible optical holder (here we use the abbreviation MCOH) for subsequent heating up to optimal for this experiment's temperature (Table I).

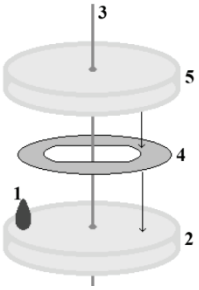

Fig. 1. The scheme of the thin-layer system heating-accelerated generation and detection.

For the spectral detection and study of the generated state, IR spectra recorded in the VTOC and the MCOH were compared with those obtained in a gas cell (for a gas phase) and for a liquid phase between optical windows at ambient conditions. The effectiveness and accuracy of the two methods used for the study of the thin-layer systems generation was previously demonstrated in our works.[7,10]

It was proved that the revealed layer is not an adsorbate or a condensate because the IR spectra of substances, evaporated into the VTOC at 6 mm thickness, disappeared after the cell thickness compression to 0.05 mm. Besides, the layer origin was tested by described heating method. The layers have been formed by the heating-accelerated evaporation into the cell with 1 mm gasket, while at the same procedure conducted with 0.2 mm gasket, the intermediate shape was not detected.

IR-spectra were recorded by IR-Fourier spectrometers IR Affinity1 (Shimadzu Co. Inc.) and FSM 1202 (InfraSpec Co. Ltd.) in 500–4000 cm^{-1} range with 2 cm^{-1} resolution and 60 scans. The spectra fragments are given in the figures with the wavenumber axis expansion according to the original record. The VTOC used was manufactured by Perkin–Elmer Co. Ltd.

The purity of the components was not less than 99.9 % as it was confirmed by chromato––mass spectrometry data obtained by GCMS–QP2010 Plus spectrometer (Shimadzu Co. Inc.).

RESULTS AND DISCUSSION

In this section, the IR results for selected aromatics, including benzene and heterocycles, are presented. We highlighted the C–H out-of-plane bending vibration (800–600 cm^{-1}) and high frequencies' (3000–2000 cm^{-1}) regions. The main manifestations of the thin layer formation could be expected in these ranges, because the first of them is sensitive to the intermolecular "stack" binding

and the second one can display the E···H (E = C, O, S or N) intermolecular binding in "chains".[17]

The most valuable results for benzene were obtained by heating of the sample between optical windows and subsequent evaporation into VTOC (see section Experimental). In the experiments with furane and thiophene, the gas–liquid systems were generated in VTOC, while for pyridine, they were obtained by heating between optical windows.

Gas–liquid system in the thin layers of benzene

The band of C–H out-of-plane bending vibration with maximum at 673 cm^{-1}, resembling the band in a gas phase (Fig. 2, spectrum A) with poorly resolved P-, Q- and R-branches, was revealed at the sample evaporation procedure in VTOC by the thickness compression from 6 to 1 mm (Fig. 2, spectrum C). At the minimal cell thickness of 0.05 mm, the C band disappears. At the thin-layer generation by heating of the sample between optical windows without a gasket, the C band of spectrum was not observed as well. Therefore, we can conclude that this band is not assigned to the adsorbed molecular layer. As the spectrum of the equilibrium gas phase cannot be observed at 1 mm optical cell thickness, the observed band can be attributed to the transient shape that appears in the thin layers and combines gas and liquid properties. The band of liquid benzene can be considered as the gas-phase band transformation through the transitional phase state band (Fig. 2, spectrum A).

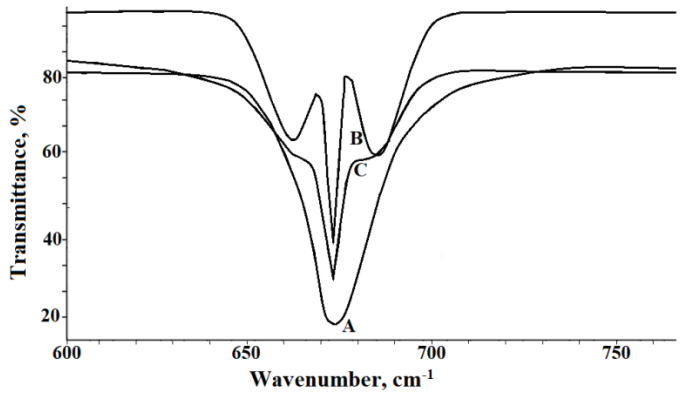

Fig. 2. Fragment of benzene spectra in C–H out-of-plane bending vibration range. Spectra: A – liquid phase; B – gas phase; C – transient phase in the thin layer.

In the spectra obtained by evaporation of the sample, placed between optical windows, with the heating to 323 K, the new bands at 654, 685 and 730 cm^{-1} were revealed (Fig. 3, spectrum B). The first two of them appears near the P- and R-branches of gaseous benzene, at 659 and 687 cm^{-1}, respectively (Fig. 3, spectrum A), while the third band is located closely to the position of the similar

mono-substituted arenes' band. The spectrum "B" after cooling transforms into the spectrum of the transitional shape, presented in Fig. 2 (spectrum C). These data can be interpreted as a manifestation of the benzene thin layer formation with the structure and binding that differ from the ones obtained in the method above by the evaporation into VTOC.

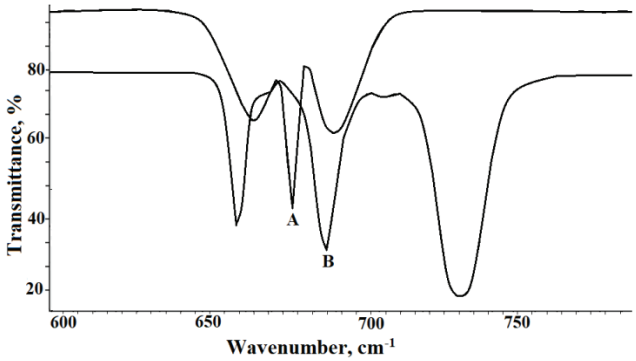

Fig. 3. Fragment of benzene spectra in C–H out-of-plane bending vibration range. Spectra: A – gaseous benzene; B – benzene transient shape in the thin layer.

Gas–liquid systems in the thin layers of thiophene and furane

In the spectra of furane, obtained at the evaporation into VTOC and subsequent lowing of the cell thickness from 6 to 1 mm, the bands at 759, 749 and 727 cm^{-1} were detected (Fig. 4A, spectrum C). The position of the central band is very close to one in the spectrum of liquid (Fig. 4A, spectrum A) and gaseous furane (Fig. 4A, spectrum B). As the spectrum of a real gas phase cannot be recorded at 1 mm cell thickness, the spectrum C can be assigned to the transient gas–liquid system of furane forming in the thin layer, as well as in the benzene spectrum above.

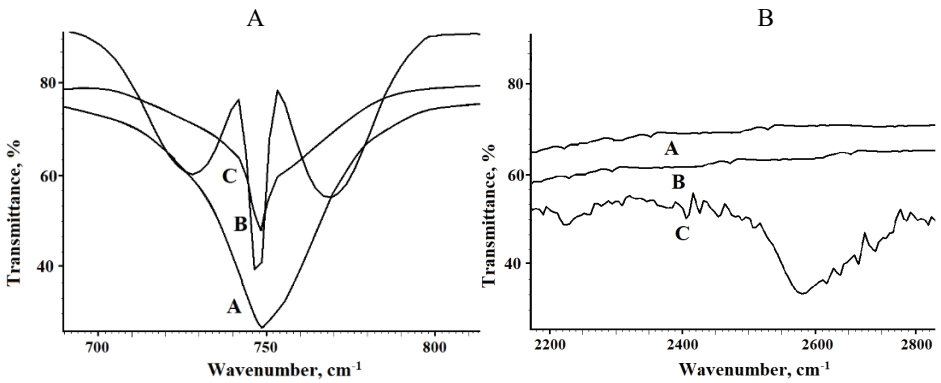

Fig. 4. Furane spectra in C–H out-of-plane bending vibration (A) and high-frequency (B) ranges. Spectra: A – liquid phase; B – gas phase, C – transient shape in the thin layer.

The new bands of the thin layer system are detected at 2598 cm^{-1}, unlike the benzene gas–liquid system (Fig. 4B, spectrum C). In the spectra of liquid and gaseous furane, these bands are absent (Fig. 4B, spectra A and B). Since this region (3600–3000 cm^{-1}) is characteristic for the O–H stretching vibrations, the revealed band can be assigned to the intermolecular O···H stretching that arises in the thin-layer gas–liquid shape.

The similar spectral picture was observed for thiophene in the C–H out-of--plane bending and the high-frequency regions (Fig. 5A). The band at 2151 cm^{-1} can be assigned to the S···H intermolecular stretching in the thin-layer gas–liquid system of thiophene (Fig. 5B).

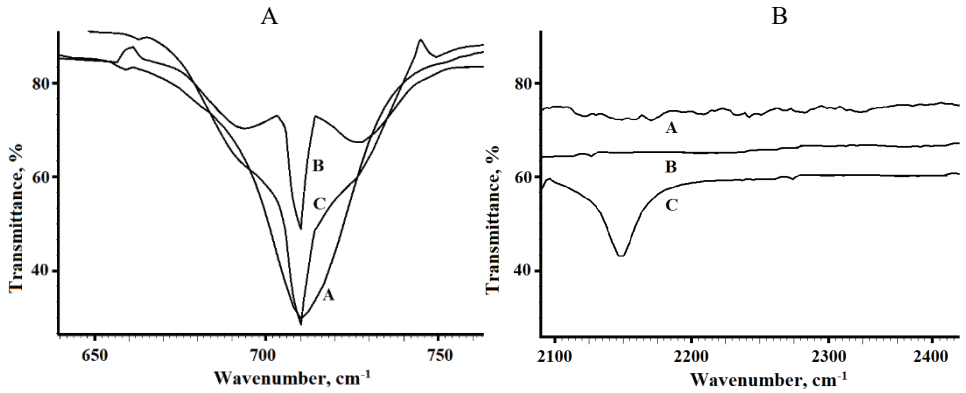

Fig. 5. Thiophene spectra in C–H out-of-plane bending vibration (A) and high-frequency (B) ranges. Spectra: A – liquid phase; B – gas phase; C – transient phase in the thin layer.

Gas–liquid system in the thin layers of pyridine

For pyridine, the generation of the thin layer system can be accomplished by heating to 373 K in the inter-window space with a 1 mm cell gasket. The observed IR absorption (Fig. 6A, spectrum B) is presented in comparison with the liquid phase (Fig. 6A, spectrum A). The spectrum of pyridine equilibrium gas phase spectrum cannot be recorded due to low volatility of the substance. However, in this case, the transition shape with dual gas-liquid spectral properties was also observed.

In the high-frequency region, a new band in the IR spectrum of the generated thin layer at 3420 cm^{-1} was observed (Fig. 6B, spectrum B). This band can be assigned to an intermolecular N···H hydrogen bond forming within an intermediate shape.

DFT modelling of intermolecular binding in the thin layers

The description of the intermolecular binding in a condensed state can be considered in terms of DFT study only as a quantitative model. It is well-known that

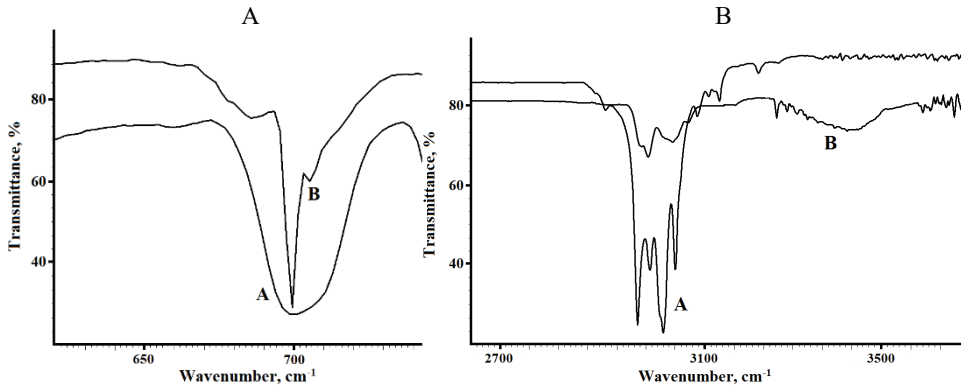

Fig. 6. Pyridine spectra in C–H out-of-plane bending vibration (A) and high-frequency (B) ranges. Spectra: A – liquid phase; B – transient phase in the thin layer.

ab initio quantum chemical calculations simulate the condensed phase for organic molecules as a set of dimers, trimers and rarely as polymolecular clusters.[3,17,18] Therefore, our effort to evaluate the intermolecular binding in the gas-liquid system of the thin layers is based on the similar conception, including the calculation of the dimer structure parameters for the different molecular shapes. The aromatics' system can exist in spatial arrangements of so called "stack" shape – with parallel and perpendicular oriented aromatic rings.[18] However, the IR data indicate the formation of the C···H interstack σ-binding as well.[17,18] The results of DFT study, in terms of the similar concept, are presented in this Section.

The calculations were caried out in terms of DFT technique with B3LYP and GD3BJ functionals[19,20] with 6–311++G (2d, 2p) basis set. For geometry optimization procedure we have used the algorithm[21]. The intermolecular distances calculated by the B3LYP functional are given in Figs. 7–10 in brackets. The additional criterium of a system geometry correct calculation is the absence of negative vibration frequencies in the final data set.

Benzene system. Two types of clusters, which represent the benzene spatial arrangement, are given in Fig. 7. DFT calculations of the optimized geometry for structure A ("stack" shape) in the variant with the B3LYP functional gives a geometry with aromatic rings arranged at an angle, so the comparison of the intermolecular bond lengths with the GD3BJ functional can be taken rather conditionally, hence the bond lengths obtained by the B3LYP functional are not given. The calculated spectral data for these structures generally agree with the experimental IR picture in CH stretching region, in which three bands are observed instead of one CH stretching band previsedfor the planar isolated ring (this problem was discussed earlier).[18] The calculations predict two bands assigning to the shape with parallel (Fig. 7A) and one band for the "T" shape (Fig. 7B). The com-

bination of these arrangement variants leads to the appearance of three bands in the spectra (Table II).

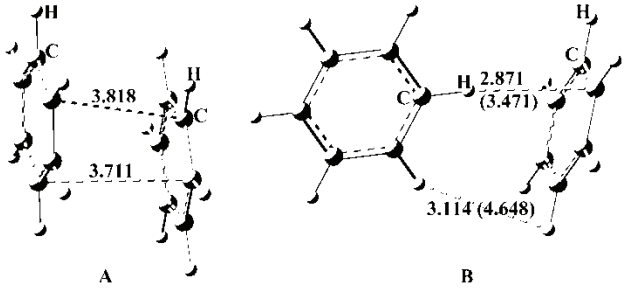

Fig. 7. Elements of spatial arrangement with optimized geometry parameters of the benzene clusters (the distances are given in Å).

The calculated IR frequencies correctly predict the existence of three bands in the CH stretching region arising due to the bands' combination of two molecular shapes – A and B.[17]

TABLE II. The experimental and calculated frequencies data of CH stretching bands

Frequencies	Wavenumber, cm^{-1}
Experimental	3092, 3071, 3036
Calculated	3122, 3053 (shape A), 3179 (shape B)

Furane and thiophene systems. For the furan molecule, the geometry optimization procedure gives two variants of σ-bonded dimers – one with the at-an--angle aromatic rings' arrangement and the intermolecular (C–C) distance of about 3.1 Å (Fig. 8A) and with the distance of about 2.7 Å (Fig. 8B). The thin--layer transient gas-liquid system, in terms of the similar model, can form under the O···H intermolecular bonded clusters with two molecular arrangement types.

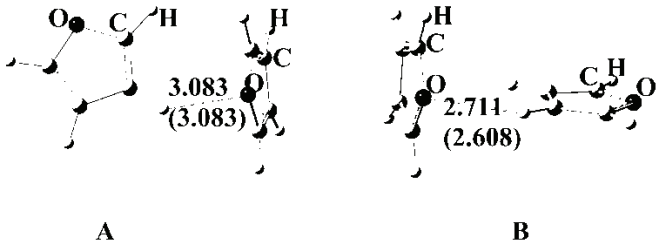

Fig. 8. Elements of spatial arrangement with optimized geometry parameters of the furan clusters (the distances are given in Å).

The structure of thiophene gas–liquid system in the thin layer predicted in DFT calculation can be presented as a state with two different shapes π-bonded

("stack" shape) and σ-bonded S···H shape (Fig. 9). In this case, DFT calculations with the B3LYP potential do not give an optimized geometry for the "stack" shape, so these values are not shown in Fig. 9.

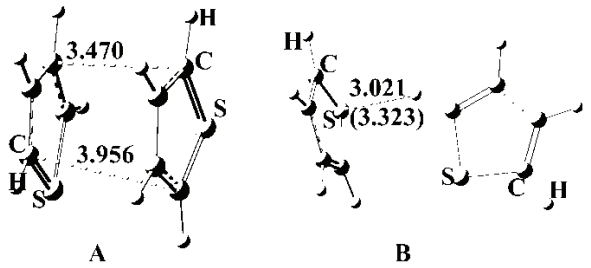

Fig. 9. Elements of spatial arrangement with optimized geometry parameters of the thiophene clusters (the distances are given in Å).

The calculated IR frequencies in CH out-of-plane bending (Q-branch only) and CH stretching ranges, where the manifestation of intermediate phase shape formation was observed, are presented in Table III (for the GD3BJ functional only). The calculated and relative experimental intensities were not listed in Table III, because these values strongly depend on the experimental conditions and do not give any useful information in terms of the considered problem.

TABLE III. The calculated and experimental IR frequencies of heterocyclic aromatics in ranges of CH out of plane bending – ρ(CH) and CH···X stretching – q(CH)

Frequencies		Wavenumber, cm^{-1}					
		C_5H_5O		C_5H_5S		C_6H_6N	
		ρ(CH)	q(CH···O)	ρ(CH)	q(CH···S)	ρ(CH)	q(CH···N)
Experimental		749	2598	709	2151	698	3420
Calculated	Shape A	756	3259	723	3253	712	3156
	Shape B	757	3259	723	3253	716	3174

Significant differences for the calculated and experimental frequencies for the CH···X stretching vibrations are probably caused by the hydrogen atom shift to the heteroatoms in the real systems.[22]

Pyridine system. The cluster structure of pyridine system predicted in the DFT study with the GD3BJ functional can be presented as a state with combination of "stack" shape (Fig. 10A) and σ- one formed under the intermolecular hydrogen N···H bond (Fig. 10B).

CONCLUSION

The presented experimental and computational data allow to make the following main conclusions.

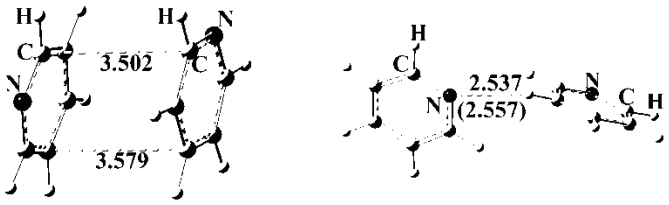

A B

Fig. 10. Elements of spatial arrangement with optimized geometry parameters of the pyridine clusters (distances are given in Å)

1. The gas–liquid systems of aromatics including heterocyclic aromatic compounds can be generated in the thin layers by evaporation and subsequent compression of the substances in VTOC, or by heating of the sample placed between optical windows and evaporation into the small inter-window space.

2. These systems manifest the dual gas–liquid spectral properties of the considered aromatics. In terms of the presented concept, their structure can be interpreted as a transient phase state arising at the liquid state transformation into the gas.

3. The spatial arrangement of the thin layers can be described as a combination of π- and σ- bonded clusters, which can simulate the gas and the liquid phase state properties. Therefore, the thin layers can be considered as an intermediate state of organic liquids.

Acknowledgement. The study was supported by Ministry of Science and Higher Education of the Russian Federation as part of the scientific project FSSM-2021-0013 of the Laboratory of Smart Materials and Technology (LSMT).

ИЗВОД

ФОРМИРАЊЕ ИНТЕРМЕДИЈАРНОГ СИСТЕМА ГАС–ТЕЧНО У ТАНКИМ СЛОЈЕВИМА АРОМАТИЧНИХ ЈЕДИЊЕЊА

ROSTISLAV V. KAPUSTIN[1], IOSIF I. GRINVALD[1], ANDREY V. VOROTYNTSEV[2], ANTON N. PETUKHOV[2,3], VLADIMIR M. VOROTYNTSEV[1], SERGEY S. SUVOROV[2] и ALEXANDRA V. BARYSCHEVA[2]

[1]Alekseev State Technical University of Nizhny Novgorod, Nizhny Novgorod, Russia, [2]Lobachevsky State University of Nizhny Novgorod, Nizhny Novgorod, Russia и [3]Dmitry Mendeleev University, Moscow, Russia

У овом раду разматрани су подаци добијени ИС спектроскопским експериментима и квантно-хемијским DFT испитивањем структуре и интермолекулских веза у интермедијерним системима гас–течно ароматичних једињења бензена, фурана, пиридина и тиофена. Ови системи могу настати у танким слојевима у близини чврсте површине применом две различите методе, у зависности од физичких особина узорка. Прва метода, која укључује исправљање а затим компресију узорка у оптичкој ћелији променљиве дебљине, је примењена на испарљива једињења: бензен, фуран и тиофен. За бензен и пиридин, коришћена је друга метода, која подразумева испаравање иницирано загревањем у затвореном простору између прозора са накнадним хлађењем узорка. Показано је да настали слој није адсорбат или кондензат. На основу ИС података добијених овим двема

методама може се закључити да добијени системи кондензованих ароматичних једињења показују дуалне гас–течно спектралне особине које могу прелазити из једних у друге у случају варирања спољних услова. Резултати DFT прорачуна показују да се просторно уређење у танким слојевима ароматичних једињења може описати као комбинација π- и σ-повезаних кластера, које симулирају особине гасне и течне фазе.

(Примљено 3. октобра, ревидирано 25 новембра, прихваћено 9. децембра 2022)

REFERENCES

1. D. B. Eremin, V. P. Ananikov, *Coord. Chem. Rev.* **346** (2017) 2 (https://dx.doi.org/10.1016/j.ccr.2016.12.021)
2. I. I. Grinvald, I. Y. Kalagaev, A. N. Petukhov, A. I. Grushevskaya, R. V. Kapustin, I. V. Vorotyntsev, *J. Struct. Chem.* **59** (2018) 313 (https://dx.doi.org/10.1134/S0022476618020087)
3. M. A. Palafox, *Phys. Sci. Rev.* **3** (2018) (https://dx.doi.org/10.1515/psr-2017-0184)
4. B. C. Smith, *Infrared Spectral Interpretation: A Systematic Approach*, 1st ed., CRC Press, Boca Raton, FL, 2018 (https://dx.doi.org/10.1201/9780203750841)
5. I. I. Grinvald, I. Y. Kalagaev, A. N. Petukhov, A. V. Vorotyntsev, R. V. Kapustin, *Struct. Chem.* **30** (2019) 1659 (https://dx.doi.org/10.1007/s11224-019-01349-2)
6. G. Szabó, D. Szieberth, L. Nyulászi, *Struct. Chem.* **26** (2015) 231 (https://dx.doi.org/10.1007/s11224-014-0543-y)
7. R. V. Kapustin, I. I. Grinvald, A. V. Vorotyntsev, A. N. Petukhov, V. I. Pryakhina, I. V. Vorotyntsev, *React. Kin. Mech. Catal.* **135** (2022) 835 (https://dx.doi.org/10.1007/s11144-022-02177-y)
8. E. S. Alekseev, A. Y. Alentiev, A. S. Belova, V. I. Bogdan, T. V. Bogdan, A. V. Bystrova, E. R. Gafarova, E. N. Golubeva, E. A. Grebenik, O. I. Gromov, V. A. Davankov, S. G. Zlotin, M. G. Kiselev, A. E. Koklin, Y. N. Kononevich, A. E. Lazhko, V. V. Lunin, S. E. Lyubimov, O. N. Martyanov, I. I. Mishanin, A. M. Muzafarov, N. S. Nesterov, A. Y. Nikolaev, R. D. Oparin, O. O. Parenago, O. P. Parenago, Y. A. Pokusaeva, I. A. Ronova, A. B. Solovieva, M. N. Temnikov, P. S. Timashev, O. V. Turova, E. V. Filatova, A. A. Philippov, A. M. Chibiryaev, A. S. Shalygin, *Russ. Chem. Rev.* **89** (2020) 1337 (https://dx.doi.org/10.1070/rcr4932)
9. N. J. Hestand, S. E. Strong, L. Shi, J. L. Skinner, *J. Chem. Phys.* **150** (2019) 054505 (https://dx.doi.org/10.1063/1.5079232)
10. I. I. Grinvald, R. V. Kapustin, *J. Serb. Chem. Soc.* **86** (2021) 1067 (https://dx.doi.org/10.2298/JSC210426048G)
11. M. I. Shakhparonov, *Contemporary Problems of Physical Chemistry*, Lomonosov Moscow State University Publishing House, Moscow, 1970
12. A. I. Abramovich, L. V. Lanshina, I. D. Kargin, *Russ. Chem. Bull.* **66** (2017) 828 (https://dx.doi.org/10.1007/s11172-017-1814-8)
13. I. D. Kargin, L. V. Lanshina, A. I. Abramovich, *Russ. J. Phys. Chem., A* **91** (2017) 1737 (https://dx.doi.org/10.1134/S003602441709014X)
14. A. I. Abramovich, *Struct. Chem.* **30** (2019) 545 (https://dx.doi.org/10.1007/s11224-019-01293-1)
15. I. I. Grinvald, I. Y. Kalagaev, A. N. Petukhov, R. V. Kapustin, *Russ. J. Phys. Chem., A* **93** (2019) 2645 (https://dx.doi.org/10.1134/S0036024419130107)

16. A. I. Abramovich, E. S. Alekseev, T. V. Bogdan, *Russ. J. Phys. Chem., A* **93** (2019) 2108 (https://dx.doi.org/10.1134/S0036024419110025)
17. I. I. Grinvald, I. Y. Kalagaev, R. V. Kapustin, in *Density Functional Theory - Recent Advances, New Perspectives and Applications*, D. Glossman-Mitnik, Ed., IntechOpen, London, 2022 (https://dx.doi.org/10.5772/intechopen.100429)
18. I. Y. Kalagaev, I. I. Grinvald, *Pure Appl. Chem.* **85** (2012) 135 (https://dx.doi.org/10.1351/PAC-CON-12-03-06)
19. S. Grimme, S. Ehrlich, L. Goerigh, *J. Comput. Chem.* **32** (2011) 1456 (https://dx.doi.org/10.1063/1.3382344)
20. D. G. A. Smith, L. A. Burns, K. Patkowsky, C. D. Sherrill, *J. Phys. Chem. Lett.* **7** (2016) 2197 (http://dx.doi.org/10.1021/acs.jpclett.6b00780)
21. R. Meyer, A. W. Hausera, *J. Chem. Phys.* **152** (2020) 084112 (https://doi.org/10.1063/1.5144603)
22. J. M. Mayer, *Acc. Chem. Res.* **44** (2011) 36 (https://dx.doi.org/10.1021/ar100093z).